ELSEVIER Journal of Electron Spectroscopy and Related Phenomena 114–116 (2001) 483–488

JOURNAL OF ELECTRON SPECTROSCOPY and Related Phenomena

www.elsevier.nl/locate/elspec

Study of electronic properties and bonding configuration at the BN/SiC interface

Hui-Qiong Wang, Jin-Cheng Zheng, A.T.S. Wee*, C.H.A. Huan

Department of Physics, National University of Singapore, Lower Kent Ridge Road, Singapore 119260, Singapore

Received 8 August 2000; received in revised form 20 September 2000; accepted 29 September 2000

Abstract

The electronic properties and bonding configuration at the interface between cubic (zinc blende) BN and 3C–SiC are studied using the first principle linear muffin-tin orbital (LMTO) method based on local-density-functional (LDA) theory. The (001) superlattice of BN(n)/SiC(n) (n=1–6) is used to study the interface. The calculated results show that the preferred bonding configuration is Si–N and C–B for the (001) BN/SiC interface. The formation energy of the interface is studied as a function of thickness of the superlattice. The origin of the bond formation as well as the electronic properties of the interface are also investigated.

Keywords: BN/SiC(001); First principle; Superlattice; Interface; Bonding configuration; Formation energy

1. Introduction

There has been increasing interest recently in wide band-gap semiconductors [1] due to their favorable properties for high temperature and electro-optical applications. Most III–V nitrides and their alloys have been shown to be promising candidates, especially for high-power and high-frequency microelectronics applications [2,3]. SiC appears to be one of the most suitable substrates for the growth of nitrides since it possesses similar thermal expansion characteristics and exhibits the same types of structural modifications, i.e. cubic (zinc blende) and hexagonal (wurtzite) structures. The interfacial properties might play an important role in understanding their applications. For nitrides, a special interest rises in BN is especially interesting because of its high thermal conductivity, large band gap, and low dielectric constants [4]. It would be useful therefore to investigate the electronic properties and bonding configuration between SiC and BN, both of which particularly possess the significant hardness.

While many theoretical calculations have been performed to investigate the cohesive and electronic properties of bulk nitrides [5–9], little has been done to study the detailed atomic structure of the nitride–substrate interfaces. Several papers have been published on the AlN/SiC, GaN/SiC [10–14] and C/BN [4,15,16] interfaces, for the reason that AlN and GaN are both well lattice-matched to SiC and C to BN. Heteroepitaxial structures with strained semiconductor thin films have found widespread applications in electronic and optoelectronic devices [17,18]. This provides strong motivation for us to

*Corresponding author. Tel.: +65-874-63-62; fax: +65-777-61-26.

E-mail address: phyweets@nus.edu.sg (A.T.S. Wee).

0368-2048/01/$ – see front matter
PII: S0368-2048(00)00365-0

study the interface between BN and SiC, which, as we will show, have an 18% mismatch. Furthermore, Lambrecht et al. [19] haves studied the electronic structure and bonding at the SiC/AlN and SiC/BP interfaces with the LMTO method. They found that the preferred bonding configurations correspond to cation–anion bonding, i.e. Si–N and C–Al for SiC/AlN, while Si–B and C–P for SiC/BP (the anomalous ion character of BP has been considered). Therefore, it would be interesting to investigate the SiC/BN interface, which involves replacing Al in SiC/AlN with B, or P in SiC/BP with N. We choose the polar (100) interface in this study to observe any differences from non-polar (110) which was chosen for their study.

In this work, the linear muffin-tin orbital (LMTO) band structure method and local-density-functional theory are used for electronic structure and total-energy calculations. We follow the common practice of using the supercell approach to study the (100) interface of SiC/BN.

2. Computation method

In our calculation, Andersen's linear muffin-tin orbital (LMTO) method [20] is used in the atomic-sphere approximation (ASA). The approach is based on the Hohenberg–Kohn–Sham density-functional method in the local-density approximation [21]. To ensure an adequate description of the potential at the tetrahedral interstitial sites, so-called empty spheres [22] are introduced to suitable sites, while preserving the crystal symmetry. It has been well established that ASA with interstitial empty spheres gives a complete description of the electronic states and ground-state properties in bulk semiconductors and at semiconductor interfaces [23,24]. The supercell approach is employed to calculate the electronic structure and properties of BN(n)/SiC(n) (n=1–5) superlattice for two bonding models, i.e. Si–N and C–B for model A, and Si–B and C–N for model B. The ultrathin superlattice 1+1 represents actually a mixed new compound, while as the cell size increases, the superlattice approaches the situation of distinguishable interface-like and bulk-like layers. After the total energy (E_{tot}) of the superlattice BN(n)/SiC(n) and the corresponding bulk materials BN and SiC have been calculated, the formation energies (E_{form}) of superlattices per atom are obtained as follows:

$$E_{\mathrm{form}}\ (\text{per atom}) = \{E_{\mathrm{tot}}[(\mathrm{SiC})_n/(\mathrm{BN})_n] - [E_{\mathrm{tot}}(\mathrm{SiC}) + E_{\mathrm{tot}}(\mathrm{BN})]^{*}n\}/4n \quad (1)$$

3. Results and discussion

3.1. Bulk structure

Firstly, we calculate the properties of pure bulk materials SiC and BN. The equilibrium lattice constants, bulk moduli and their pressure derivative and cohesive energies as well as other available results are summarized in Table 1. We performed the calculation of total energy as a function of lattice constant in a range of about 5% expansion and compression and the result is fitted to the universal energy relation of Vinet et al. [25]. The results are in excellent agreement with experimental data and other

Table 1
Equilibrium lattice constant, bulk modulus, and its pressure derivative and cohesive energy for cubic SiC and BN

	Reference	a (Å)	B (GPa)	B'	E_{coh} (eV/pair)
SiC	This work	4.40	257	2.8	13.26
	(theory) [18]	4.32	233	3.8	14.06
	(exp.)	4.3596 [26]	224 [27]	–	12.68 [28]
BN	This work	3.61	392	3.79	15.44
	(theory)	3.58 [4], 3.606 [29]	412 [4], 367 [29]	3.6 [4]	15.8 [4], 14.3 [29]
	(exp.)	3.617 [30], 3.616 [31]	290 [4][a], 465 [32][a], 369 [33]	–	13.2 [28][b]

[a] From estimated elastic constants.
[b] From energies of formation of this reference.

theoretical results. This, to some extent, calibrates the accuracy of the calculation method used.

3.2. Bonding configuration

To identify the favorable model of bonding configuration, the same calculation method of total energy as a function of lattice constant mentioned in Section 3.1 has been applied to the BN/SiC(100) interface with ultrathin (1+1) superlattice. The results for the two kinds of bonding models are presented in Fig. 1. It can be is clearly seen that the total energy for model A (formation energy of 0.62 eV/atom) is much lower than that for model B (formation energy of 2.38 eV/atom), which indicates that model A is more stable than model B. Since the (1+1) superlattice is a truly mixed compound and not really meaningful as a representation of the interface structure, we increase the thickness of the superlattice step by step to identify the interface properties. The result of equilibrium lattice constant as a function of thickness can be seen in Fig. 2. It is interesting to find that model A quickly arrives at the stable lattice constant of 4.09 Å from $n=2$, and only

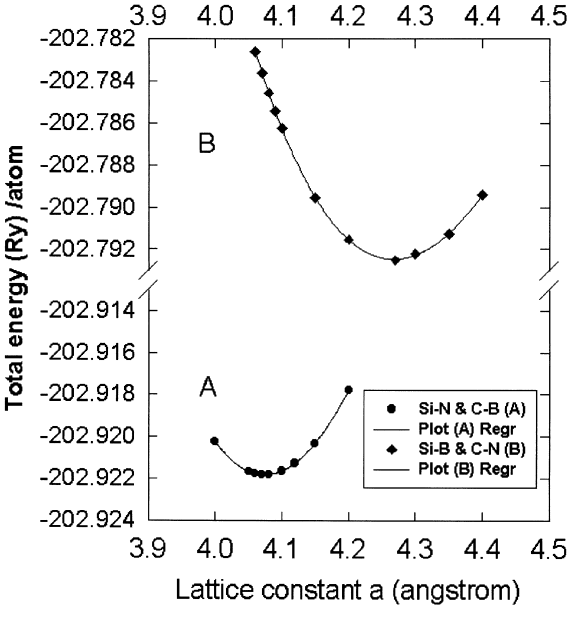

Fig. 1. Total energy as a function of lattice constant for (1+1) SiC/BN.

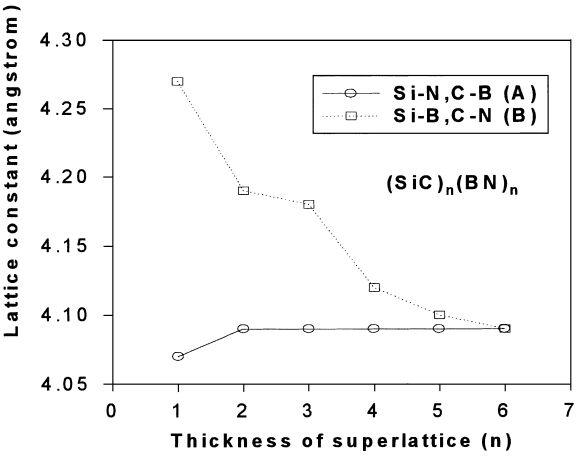

Fig. 2. Equilibrium lattice constant as a function of superlattice thickness n.

the lattice constant at $n=1$ has a slightly smaller equilibrium lattice constant. However, model B shows a large variation in lattice constant until it finally reaches 4.09 Å. This effect can be understood since for model B, the bonding is unstable, resulting in charge transfer from the interface to the bulk layers. For SL(1+1), the wrong bonding results in large electrostatic energy, so it trends to enlarge the geometry of the SL to reduce electrostatic energy. This explains why the lattice constant of model B (SL1+1) is larger than that of model A. When n increases, the lattice constant approaches to be 4.09 Å because the electrostatic energy has been reduced by charge transfer from the interface to the bulk layers. It is expected that these two models should eventually reach the same equilibrium lattice constant, since when $n=6$, the superlattice contains almost bulk-like material.

Our conclusion that Si–N and C–B forms the preferred bonding configuration agrees with the result of SiC/AlN(110) by Lambrecht et al. [19] as well as that of GaN/Si(001) and AlN/SiC(001) reported by Städele et al. [10]. These results all show that the preferred bonding configurations correspond to cation–anion bonding. In order to investigate the detailed information about how Si–N and C–B forms the favorable bonding configuration, we calculate the charge distribution per atomic layer. Table 2 lists the results for bulk SiC, BN as well as the (1+1) and (5+5) superlattices of SiC/BN. One can

Table 2
Charges (in units of $|e|$) per atomic layer

SiC (bulk)		BN (bulk)		SL(1+1)A		SL(1+1)B		SL(5+5)A		SL(5+5)B	
Si	1.166	B	0.243	Si	1.402	Si	1.101	Si(3)[a]	1.197	Si(3)[a]	1.196
C	−1.166	N	−0.243	C	−0.759	C	−0.423	C(3)[a]	−1.197	C(3)[a]	−1.197
				B	0.158	N	−0.316	Si(2)	1.195	Si(2)	1.191
				N	−0.801	B	−0.384	C(2)	−1.218	C(2)	−1.224
								Si(1)	1.226	Si(1)	1.238
								C(1)	−0.722	C(1)	−0.501
								B(1)	0.217	N(1)	−0.323
								N(1)	−0.360	B(1)	0.412
								B(2)	0.391	N(2)	−0.373
								N(2)	−0.378	B(2)	0.376
								B(3)[a]	0.377	N(3)[a]	−0.381
								N(3)[a]	−0.377	B(3)[a]	0.378

[a] n in Si(n) or C(n) means the layer numbers counted from interface layer. Si(3) and C(3) are central layers for SiC part of $(SiC)_5/(BN)_5$.

see that for the (5+5) superlattice, the charge in the central layer (the 3rd layers from the interface) has nearly reached the bulk equilibrium values. This means $n=5$ is large enough for the central layer of the superlattice to exhibit bulk properties. Thus, the interface layer in the (5+5) unit cell can represent the real interface layer. It can be seen that the charge distribution is different between models A and B. Model A appears to be more ionic, while model B is more covalent, thereby possessing more electrostatic energy. Furthermore, we also calculated the electronegativities for elements of BN–SiC and the difference in electronegativities for models A and B, and the results are shown in Table 3. It can be seen that the total difference in electronegativities of model A is much larger than that of model B. This means that atoms in model A combine more tightly to each other making it more stable.

Table 3
Electronegativity (S) [34] for elements of SiC–BN and difference in electronegativities (ΔS) for models A and B

Electronegativity (S) [34]				Difference in electronegativities (ΔS) A model		B model	
B	N	Si	C	Si–N	C–B	Si–B	C–N
2.93	4.49	2.84	3.79	1.65	0.86	0.09	0.70
Total	–	–	–		2.51		0.79

3.3. Formation energy

We also calculate the results of formation energies of (BN)n/(SiC)n as a function of superlattice thickness n. The formation energy is normalized as the energy of formation per atom using the equation (1) in Section 2. Some interesting conclusions can be derived from the plot of formation energy against the increase of superlattice thickness (Fig. 3). The formation energy is normally found to be monotoni-

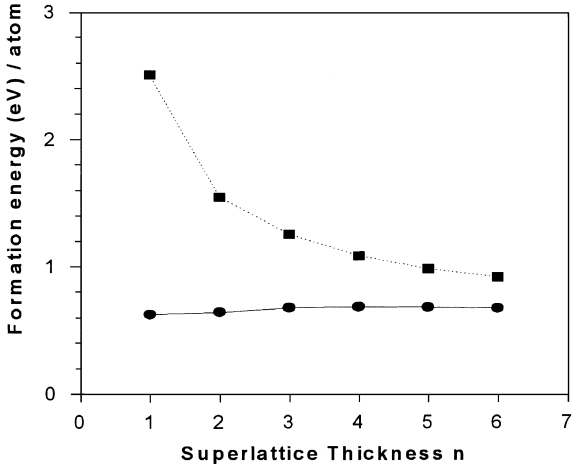

Fig. 3. Formation energy as a function of superlattice thickness n.

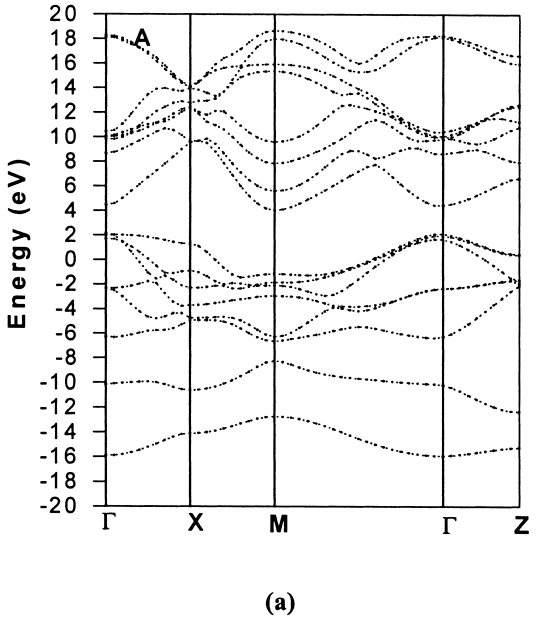

(a)

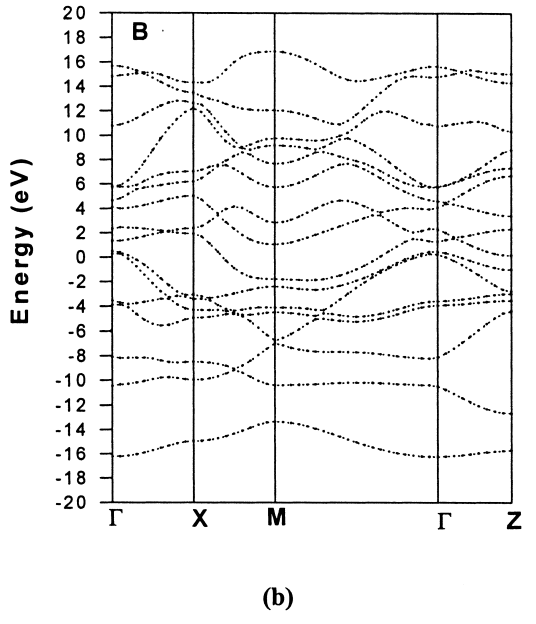

(b)

Fig. 4. Band structure of SiC/BN(001) (1+1) superlattice for model A (a) and model B (b).

cally decreasing as shown for model B, but for model A, there exits a maximum formation energy at $n=4$, i.e. the formation energy increases when n increases from 1 to 4, but decreases when n changes from 4 to 6. The latter is a normal trend as explained above. However, the unusual trend of n increasing from 1 to 4 suggests that the SL (1+1) of Si–N and C–B bonding model is actually a stable or at least metastable new compound. The behavior of formation energy as a function of thickness of SL indicates that it is energetically more favorable to form the thinner (1+1) superlattice rather than segregating into thicker SiC and BN layers. We note from Fig. 2 that the smallest equilibrium lattice constant of SL($n+n$) is SL(1+1) of model A. This can be explained from the analysis of formation energy. Since the formation energy of SL(1+1) (model A) is the smallest (namely, binding energy is the largest), the larger binding energy will lead to a shorter bond length. The smaller bond length of SL(1+1) supports the postulate that SL(1+1) may be a metastable or stable structure.

3.4. Electronic properties

To investigate the effect of different bonding configurations on electronic properties, the band structure computation is also carried out for these two models. As we can see from Fig. 4a and b, model A shows characteristics of a semiconductor, while for model B, the band structure exhibits anomalously metallic properties. For model B, the interface localized states occur in the main band gap. This pushes the Fermi level up and the bands shift upward. This behavior is very similar to that of SiC/AlN with unfavorable bonding configuration, Si–B and C–N [19]. In a result, model B is unfavorable not only because of the electrostatic contribution but also in terms of the band-structure component.

4. Conclusion

In conclusion, we present the results for the electronic structures and total-energy properties of the BN/SiC(100) interface as well as cubic bulk BN

and SiC. We find that the favorable bonding configuration is Si–N and C–B, which corresponds to cation–anion bonding. In our paper, the formation energy as a function of the thickness of superlattice is also investigated. The origin of the bond formation and the stability of the new compound BN–SiC are also discussed.

Acknowledgements

The authors Hui-Qiong Wang and Jin-Cheng Zheng thank Professor Renzhi Wang in the Department of Physics, Xiamen University, China for helpful discussions.

References

[1] J.T. Glass, R. Messier, N. Fujimori (Eds.), Diamond, Boron Nitride, Silicon Carbide and Related Wide Bandgap Semiconductors, MRS Symposia Proceedings No. 162, Materials Research Society, Pittsburgh, 1990.
[2] S. Strite, M.E. Lin, H. Morkoc, Thin Solid Films 231 (1993) 197.
[3] H. Morkoc, S. Strite, G.B. Cao, M.E. Lin, B. Sverdlov, M. Burns, J. Appl. Phys 76 (1994) 1363, and references therein.
[4] W.R.L. Lambrecht, B. Segall, Phys. Rev. B 40 (1989) 9909, and references therein.
[5] K. Kim, W.R.L. Lambrecht, B. Segall, Phys. Rev. B 50 (1994) 1502.
[6] A. Rubio, J.L. Corkill, M.L. Cohen, E.L. Shirley, S.G. Louie, Phys. Rev. B 48 (1993) 11810.
[7] P.E. Van Camp, V.E. Van Doren, J.T. Devreese, Phys. Rev. B 44 (1994) 9056.
[8] M. Suzuki, T. Uenoyama, A. Yanase, Phys. Rev. B 52 (1995) 8132.
[9] S.H. Wei, A. Zunger, Appl. Phys. Lett. 69 (1996) 2719.
[10] M. Städele, J.A. Majewski, P. Vogl, Phys. Rev. B 56 (1997) 6911.
[11] S.Y. Ren, J.D. Dow, Appl. Phys. Lett. 69 (1996) 251.
[12] K. Nath, A.B. Anderson, Phys. Rev. B 40 (1989) 7916.
[13] L.K. Teles, L.M.R. Scofaro, R. Enderlein, J.R. Leite, A.J. Osiek, D. Schikora, K. Lischka, J. Appl. Phys. 80 (1996) 6322.
[14] R. Di Felice, C.M. Bertoni, A. Catellani, Appl. Phys. Lett. 74 (1999) 2137.
[15] J.C. Zheng, C.H.A. Huan, A.T.S. Wee, R.Z. Wang, Y.M. Zheng, J. Phys.: Condens. Matter 11 (1999) 927.
[16] Y.M. Zheng, R.Z. Wang, J.C. Zheng, G.M. He, J. Xiamen Univ. (Nat. Sci) 35 (1996) 705, in Chinese.
[17] P. Kordos, J. Novak, Hetero-structure Epitaxy and Devices, Kluwer, Boston, 1998.
[18] T.P. Pearsall, Strain Layer Super-lattices, Academic Press, Boston, 1990.
[19] W.R.L. Lambrecht, B. Segall, Phys. Rev. B 43 (1991) 7070.
[20] O.K. Anderson, Phys. Rev. B 12 (1975) 3060.
[21] P. Hohenberg, W. Kohn, Phys. Rev. B. 136 (1964) 864.
[22] D. Glötzel, B. Segall, O.K. Andersen, Solid State Commun. 36 (1980) 403.
[23] N.E. Christensen, Phys. Rev. B 37 (1988) 4528.
[24] W.R.L. Lambrecht, B. Segall, Phys. Rev. Lett. 61 (1988) 1764.
[25] P. Vinet, J. Ferrante, J.R. Smith, J.H. Rose, J. Phys. C 19 (1986) L467.
[26] O. Madelung, M. Schulz, H. Weiss (Eds.), Physics of Group IV Elements and III–V Compounds, Landolt–Bornstein Tables, Vol. 17a, Springer, Berlin, 1982, and references therein.
[27] D.H. Yean, J.R. Riter Jr., J. Phys. Chem. Solids 32 (1971) 653.
[28] D.D. Wagman, W.H. Evanx, V.B. Parker, I. Halow, S.M. Baily, R.H. Schumm (Eds.), Selected Values of Chemical Thermodynamics Properties. Tables for the First Thirty-Four Elements in the Standard Order of Arrangement, National Bureau of Standards, Technical Note No. 270-3, US GPO, Washington, DC, 1968.
[29] R.M. Wentzcovitch, K.J. Chang, M.L. Cohen, Phys. Rev. B 34 (1986) 1071.
[30] E. Knittle, R.B. Kaner, R. Jeanloz, M.L. Cohen, Phys. Rev. B 51 (1995) 12149.
[31] O. Madelung (Ed.), Landolt–Börnstein: Numerical Data and Functional Relationships in Science and Technology, New Series, Vol. 17a, 1982.
[32] J.A. Sanjuro, E. López-Cruz, P. Vogl, M. Cardona, Phys. Rev. B 28 (1983) 4579.
[33] E. Knittle, R.M. Wentzcovich, R. Jeanloz, M.L. Cohen, Nature 337 (1989) 349.
[34] R.T. Sanderson, Chemical Bonds and Bond Energy, Academic Press, New York, 1976, Chapter 2.